Hydrogenolysis of Empty Fruit Bunch Over Cerium Supported Mesoporous Silica Catalyst

Fildzah Ariffin[1], Sugeng Triwahyono[1], Jahimin Asik[2#]

1 Department of Chemistry, Faculty of Science, Universiti Teknologi Malaysia, 81310 UTM Johor Bahru, Johor, MALAYSIA.
2 Faculty of Science and Natural Resources, Universiti Malaysia Sabah, Jalan UMS, 88400 Kota Kinabalu, Sabah, MALAYSIA.
#Corresponding author. E-mail: jthan@ums.edu.my; Tel: +6088-320000; Fax: +6088-435324.

ABSTRACT Hydrogenolysis of EFB into hydrocarbon and phenolic compounds were successfully carried out at different reaction pressure using acid catalyst of 10Ce-MeSiC. From the GC-MS analysis it showed the main composition of hydrogenolysis of lignin was phenol. However, increasing the reaction pressure to 12 bars, increased the selectivity of hydrocarbon with value 23.31% while the phenol conversion was 26.50%. Cyclopentadecane hydrocarbon appears as a main composition in alicyclic hydrocarbon. While, phenol, 2-methoxy- and phenol, 2,6-dimethoxy- was appears as a phenol derivatives compound.

KEYWORDS: Hydrogenolysis; Empty fruit bunch; Cerium; Hydrocarbon; Phenol
Received 17 August 2022 **Revised** 5 September 2022 **Accepted** 9 September 2022 **Online** 26 October 2022

Original Article

INTRODUCTION

Hydrogenolysis of biomass is recognized as an efficient and feasible process to selectively convert lignocellulose into a fuel and value-added chemicals. This process is an effective method for breaking the intermolecular linkages between lignin and cellulose/hemicellulose, as well as the intramolecular linkages in lignin (Nakagawa & Keiichi, 2012). Empty fruit bunch (EFB) consists of 60% of cellulose and hemicelluloses. EFB is a major waste of palm oil industry. This cellulose can be converted into biofuels and variety types of chemicals via various types of chemical reaction (Kim *et al*. 2017). Catalytic hydrolysis, solvolysis, liquefaction, pyrolysis, gasification, hydrogenolysis and hydrogenation are the major processes of converting lignocellulosic biomass into biofuels. Regarding catalytic hydrolysis, the acid catalysts cover inorganic or organic acids and various solid acids such as sulfonated carbon, zeolites, heteropolyacids and oxides. Liquefaction and fast pyrolysis of cellulose are primarily conducted over catalysts with proper acidity/basicity (Besson *et al.* 2013). The motivation behind this work is to convert EFB into phenolic and hydrocarbon compounds, assisted by Ce-mesoporous silica catalyst in high pressure autoclave. In this process, the reaction conditions, solvents and catalysts are the prime factors that affect the yield and composition of the target products.

METHODOLOGY

Materials

Empty fruit bunch (EFB) fibers with average particles size 4 – 5 mm was preheated at 110°C for 12 hours in a ventilated oven to remove the moisture prior to experiment.

Synthesis of Mesoporous Silica Catalyst (MeSiC)

In a typical synthesis, tetraethyl orthosilicate (TEOS, 2.5 g, 0.012 mol) was dissolved in a solution of cyclohexane (30 ml) and pentanol (1.5 ml). Mix the solution of cetylpyridinium bromide (CPB; 1 g, 0.0026 Mol) and urea (0.6 g, 0.01 Mol) in water (30 ml). The mixture was stirred for 30 min at room temperature, and the resulting solution pour into Teflon-sealed microwave (MW) reactor. The mixture was exposes to MW irradiation at 120°C for 4 hours. After completion of the reaction, the

mixture was cool at room temperature and then the silica formed was centrifuged and washed with cool distilled water and acetone. Next, the sample was dried for 24 hours and calcined at 550 °C for 6 hours under air (Moon & Lee, 2012; Dhiman & Polshettiwar, 2015).

Catalyst Preparation

The 10 wt.% of Ce-MeSiC was prepared using wet impregnation method. In a typical preparation, nitrate metal (Sigma-Aldrich) was dissolved in deionized water, and a known amount of powder support was added into the slurry. After 2 hours of rotation for homogenization, the water was removed by evaporation at 80 °C under vacuum. The slurry was dried at 110 °C for 12 h and calcined at 550 °C for 6 hours under air (Jamil *et al.* 2009; Idris & Hamid, 2009). The prepared catalysts are denoted as 10Ce-MeSiC.

Hydrogenolysis Process

The hydrogenolysis process was carried out in a 500 mL high pressure stainless steel reactor. About, 0.2 g of catalyst were reduced by H_2 at 200 °C for 2 h. Then, 10 grams of EFB fiber with appropriate solvent was rapidly introduced into the autoclave. The autoclave was then sealed and purged with nitrogen and then pressurized to the desired hydrogen pressure. The reaction was optimized by varying the reaction pressure ranging from 4 to 14 bars at fixed temperature of 120°C and held for 10 h until the reaction complete. After the reaction, the autoclave allowed to cool down to room temperature, and pressure was brought down to ambient pressure. The liquid samples were then collected and analyzed using the GCMS-FID and the char was dried in the oven. The conversion was determined by using Equation (1) as follows (Edake *et al.* 2017):

$$Conversion\ (\%) = \left(1 - \frac{weigh\ of\ unreacted\ biomass\ (g)}{weight\ of\ charged\ biomass\ (g)}\right) \text{x } 100 \qquad (1)$$

Characterization

The thermal properties of fresh EFB and catalysts were determined using a TGA (Mettler-Toledo TG50). The materials were heated from 50 - 700 °C at heating rate 10 °C min^{-1} in a N_2 atmosphere with a flow rate of 30 ml min^{-1}. The nitrogen physisorption analysis of the catalysts was carried out by using a Micromeritics ASAP 2020. Prior to the measurement, the catalyst was put into a sample tube holder, followed by evacuation at 573 K for 1 h. Then, adsorption of nitrogen was carried out at 77 K. Surface area, pore size distributions and pore volumes were determined from the sorption isotherms using a non-local density functional theory (NLDFT) method. The crystalline structure of the catalyst was studied by X-ray diffraction (XRD) recorded on a Bruker Advance D8 X-ray powder diffractometer (40 kV, 40 mA) using Cu Kα radiation source in the range of 2θ = 2–90° with a scan rate of 0.1° continuously. The surface morphology of the samples was performed using scanning electron microcopy (JEOL JSM-6390LV) working at 15 kV.

Analysis of Liquid Product

The chemical composition of the liquid oil was analyzed using a gas chromatography-mass spectroscopy-flame ionization detector (Agilent Technologies 6890) with a HP-5MS capillary column of 30 m in length and 250 ⌀m in diameter. The GC oven temperature was raised from the initial temperature of 90 to 280°C min^{-1} and was held constant for ~10 min, while the helium gas flow rate supplied to the GC was maintained at 2 mL min^{-1}. The gas chromatograph was connected to a mass spectroscopy (MS) (Agilent Technologies 5975 series) equipped with an inert mass selective Detector (MSD) at scanning acquisition mode. The mass spectroscopy was set to electron ionization mode with the ion source temperature of 230°C, emission current of 34.6 ⌀A, ionization energy of 70 eV, full scan range of 50 to 550 and quantization by selected ion monitoring mode. The Agilent Chemstation software was used to identify the chemical compounds and peaks with the help of

NIST library. It is noted here that only compounds with match factor of greater than 90% were considered.

RESULT AND DISCUSSION

Characteristics of Empty Fruit Bunch (EFB)

The TGA analysis shows that the moisture content of the EFB approximately 3.56 wt.%, while the volatile, fixed carbon, and ash contents are 54.93, 26.44, and 15.07 wt.%, respectively. The elemental analysis result showed carbon content of 38.82 wt.%, followed by oxygen (26.70 wt.%), nitrogen (0.35 wt.%), sulphur (15.80 wt.%) and hydrogen (3.71 wt.%), while their thermal degradation behaviour is shown in Figure 1(a). From the TGA-DTG profile, the sample started to decompose above 150°C and became significant at 180°C with increasing rate. The process was terminated at 550°C after weight loss of approximately 80.0 %. The DTG results thermal decomposed started at 180 to 400°C, which appears as a stiff shoulder peak. The same degradation thermal behaviour of EFB has also been observed from previous study (Parshetti *et al.* 2014).

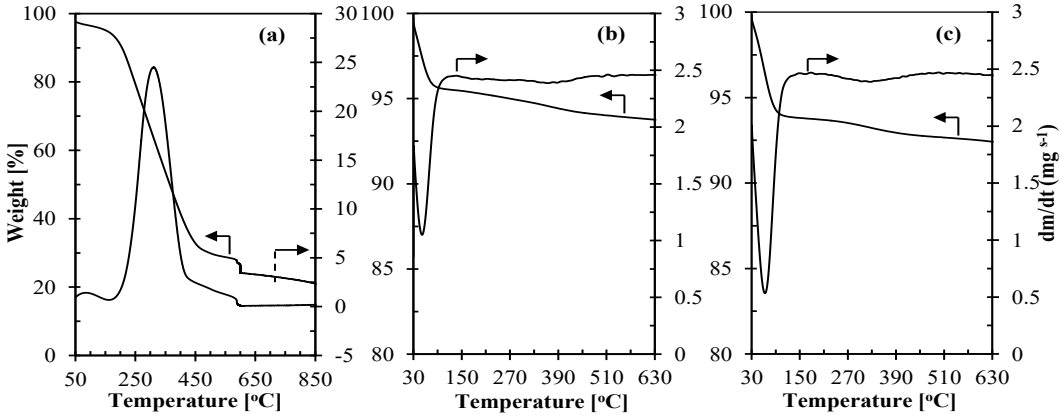

Figure 1. TGA-DTG profiles of (a) fresh EFB, (b) bare MeSiC and (c) 10Ce-MeSiC

The TGA-DTG profile of bare MeSiC (Figure 1(b)) and 10Ce-MeSiC (Figure 1(c)) are clearly shows that the bare MeSiC and 10Ce-MeSiC catalysts have high oxidation temperature with approximate weight loss of 10.0 wt.% at high temperature (650°C). From the DTG profile it shows a sharp and long peak of water evaporation occur at temperature range 30 – 150°C. This is due to high surface area and large pore diameter of the catalyst (Figure 2(a) and 2(b)) which can trap more moisture onto the pore of the catalyst.

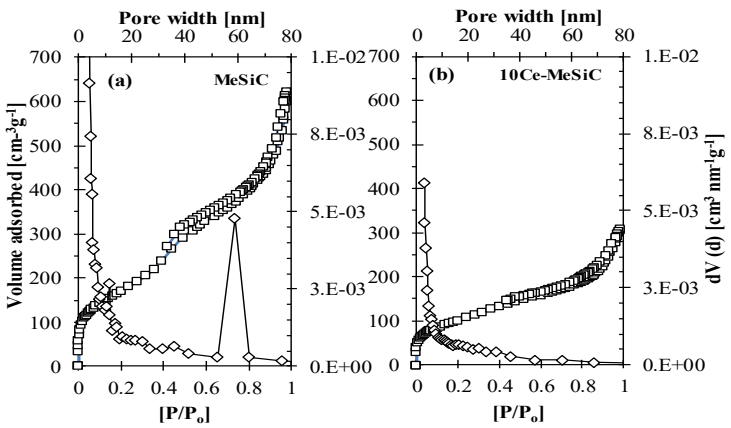

Figure 2. BET surface area of (a) bare MeSiC, (b) 10Ce-MeSiC catalysts.

The N_2 adsorption–desorption isotherm of bare MeSiC and 10Ce-MeSiC catalysts is shown in Figure 2(a) and 2(b). The average surface area of bare MeSiC catalyst was 623.87 m^2g^{-1}. After adding cerium metal onto the catalyst surface, the surface area drops to 371.56 m^2g^{-1}. Both catalysts isotherms showed a type IV and type H1 hysteresis loops, indicated of mesoporous materials with highly uniform pores. Two steps of capillary condensation were revealed at first step P/P_o=0.3 which projected to mesopores structured inside the catalysts (intraparticle) (Moon & Lee, 2012; Dhiman & Polshettiwar, 2015). At a higher partial pressure (P/P_o= 0.9), a small hysteresis loop was observed in MeSiC and 10Ce-MeSiC catalysts, which assigned to interparticle textural porosity. This indirectly reflects to the size of molecules, i.e. a higher partial pressure and linked with a smaller particle size.

The crystallinity of bare MeSiC and 10-MeSiC catalysts in Figure 3(a) and 3(b) show one broad peak at 2θ ≈ 23° for bare MeSiC and two broad peaks at ≈ 23° and 33° observed in 10Ce-MeSiC catalyst. This demonstrating that both catalysts are an amorphous mesostructured catalyst (JCPDS No. 29- 0085) (Parshetti *et al.* 2014).

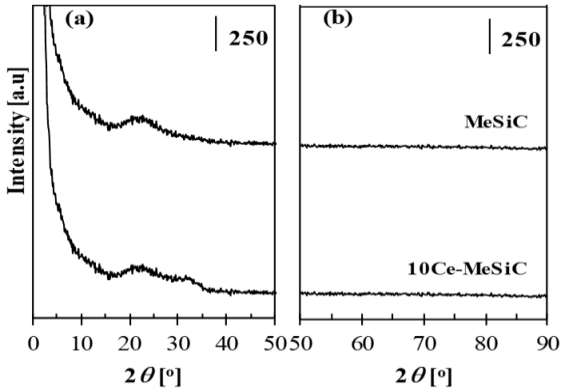

Figure 3. XRD pattern of (a) short and (b) long angle of bare MeSiC 10Ce-MeSiC catalysts.

The FESEM micrographs of EFB reveal the fiber surface characteristics and fine structure of the cellulose (Figure 4). The microfibril surface of biomass was relatively smooth surface structure (Figure 4(a)). While, at high magnification (Figure 4(b)), it showed a small hole on the biomass surface indicated the non-porosity of cellulose.

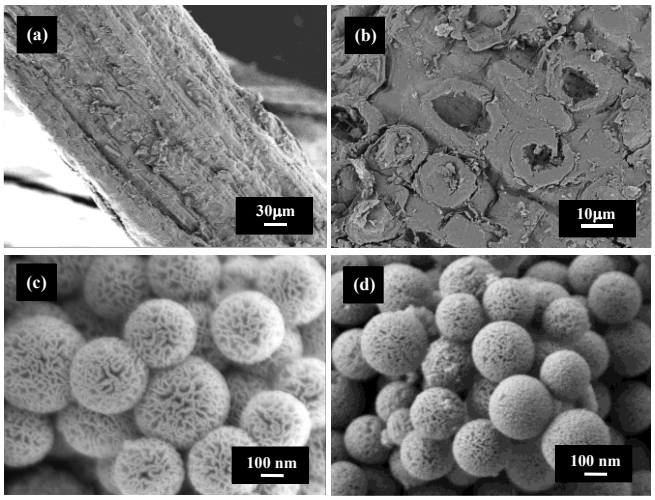

Figure 4. FESEM images of (a, b) EFB at low and high magnification, (c) bare MeSiC and (d) 10Ce-MeSiC catalysts.

For the mesoporous silica catalyst, it showed both (before and after Ce-metal loading) catalysts have uniform wrinkle-like structure with an average diameter in the range of 400-500 nm. It showed the Ce-metal catalyst does not destroy the mesoporous structure of the catalyst.

Catalytic Performance

The chemicals composition of liquid product is shown in Fig. 5, while Table 2 shows the detail of chemicals composition present during the hydrogenolysis of EFB at different reaction pressure. About 11 chemical components were detected by GC-MS (match factor > 90%) as listed in Table 2. From the Fig. 5a, it clearly shows that lower pressure (4 bars) gives lower conversion with value 41.26 wt.%, and as the pressure increased to 8 bars the conversion was increased to 89.35 wt.%. The highest conversion was achieved at pressure 10 bars with value 97.21 % and reach equilibrium after reaction at pressure 12 bars.

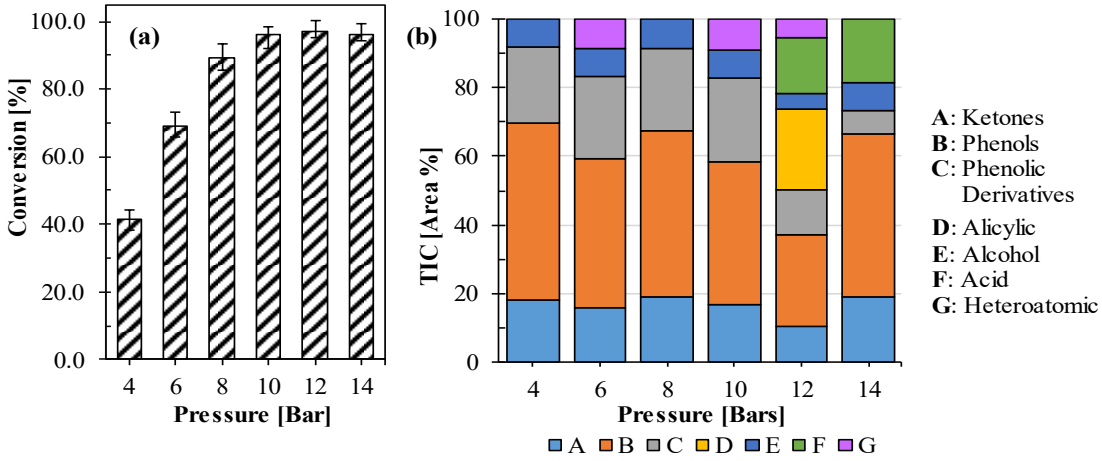

Figure 5. (a) Catalytic conversion of hydrogenolysis EFB under different reaction pressure and (b) chemicals selectivity towards different reaction pressure.

Table 2. Chemical components distribution from hydrogenolysis EFB under different reaction pressure (bars).

RT	Library/ID	4	6	8	10	12	14
4.03	1-Hydroxy-2-butanone	10.77	9.18	11.73	9.76	6.25	11.60
6.15	Pyrazole, 1,4-dimethyl-	0.00	8.62	0.00	8.87	5.59	0.00
7.10	2-Furanmethanol	7.89	7.88	8.51	8.21	4.77	7.96
11.92	Phenol	51.92	43.42	48.47	41.85	26.50	47.26
13.24	2-Cyclopenten-1-one,	7.13	6.80	7.26	6.77	4.14	7.47
15.34	Phenol, 2-methoxy-	6.66	6.19	7.01	6.02	3.85	0.00
18.88	1,2-Benzenediol	0.00	4.01	0.00	3.50	0.00	0.00
22.98	Phenol, 2,6-dimethoxy-	15.62	13.91	17.03	15.02	9.62	7.12
52.18	4-Trifluoromethylbenzoic acid. 4-hexadecyl ester	0.00	0.00	0.00	0.00	6.44	18.59
58.68	cis-11,14-Eicosadienoic acid, methyl ester	0.00	0.00	0.00	0.00	9.54	0.00
61.69	Cyclopentadecane	0.00	0.00	0.00	0.00	23.31	0.00

The detail of chemicals composition derived from every sample was revealed in Fig 5b. From the Figure, it showed the main composition in liquid product is phenolic compounds. At lower pressure (4 bars) highest conversion of phenols was observed with value 51.92 %, followed by 8 bars reaction pressure with value 48.47 %. However, when the pressure increased to 10 bars the conversion decreased to 26.50 %. Interestingly, the reaction at pressure 12 bars produced higher hydrocarbon fraction with value 23.31%. It showed an optimised reaction pressure to produced fuels and value-added chemicals can achieved at pressure 12 bars. As indicated in Figure 5(b), there are seven types of products were produced which are ketones, phenol, phenolic compounds, alkanes, alcohol, acids and heteroatomic compounds. Phenolic compounds comprised of 1,2-benzenediol, phenol, 2,6-dimethoxy- and phenol, 2-methoxy-; while alcohol compounds consist of 2-furanmethanol. While

hydrocarbon appears in the form of Cyclopentadecane. The process also can be achieved by the pyrolysis of EFB using microwave (Ali & Idris, 2016). Other compounds such as ketones compounds present equally in each reaction pressure.

CONCLUSION

The catalytic conversion of EFB towards hydrocarbon and phenolic compounds was successfully optimized at different reaction pressure. From the results it showed the main composition of hydrogenolysis of lignin was phenol which was optimum at 8 bars. However, higher selectivity conversion toward hydrocarbon compounds can be achieved by increasing the reaction pressure to 12 bars. Overall, this paper showed Ce-MeSiC improved the conversion of lignin into hydrocarbon and phenol.

ACKNOWLEDGEMENT

This research was supported by Universiti Malaysia Sabah under grant number RACE16-TK-2014.

REFERENCES

[1] Ali, A. & Idris, R. 2016. Utilization of low-cost activated carbon from rapid synthesis of microwave pyrolysis for WC nanoparticles preparation. *Advanced Materials Letters*, 8(1), 70-76.

[2] Besson, M., Gallezot, P. & Pinel, C. 2013. Conversion of biomass into chemicals over metal catalysts. *Chemical Reviews,* 114(3), 1827-1870.

[3] Dhiman, M., Chalke, B. & Polshettiwar, V. 2015. Efficient synthesis of monodisperse metal (Rh, Ru, Pd) nanoparticles supported on fibrous nanosilica (KCC-1) for catalysis. *ACS Sustainable Chemistry & Engineering*, 3(12), 3224-3230.

[4] Edake, M., Dalila, M., Mahboub, M.J.D., Dubois, J-L. & Patience, G.S. 2017. Catalytic glycerol hydrogenolysis to 1,3-propanediol in a gas–solid fluidized bed. *Royal Society of Chemistry*, 7, 3853-3860.

[5] Idris, R. & Hamid, S. A. 2009. Thermal behavior study of the MoVTeNb oxide catalyst for selective oxidation process. *AIP Conference Proceedings in International Conference on Nanoscience and Nanotechnology (NANO-SciTech 2008)*. 18-21 November 2008, Selangor, Malaysia. pp. 16-20.

[6] Jamil, A.A., Idris, R., Asik, J., Bernard, B.B., Gindana, B. & Tan, F. 2015. Comparative Study Based on Activation Procedure Using Air and Nitrogen Gas to Synthesis Nanoparticles Cu/Al_2O_3 Catalyst. *Advanced Materials Research*, 1107, 96-100.

[7] Kim, M., Son, D., Choi, J. W., Jae, J., Suh, D. J., Ha, J. M. & Lee, K. Y. 2017. Production of phenolic hydrocarbons using catalytic depolymerization of empty fruit bunch (EFB)-derived organosolv lignin on Hβ-supported Ru. *Chemical Engineering Journal*, 309, 187-196.

[8] Kobayashi, H., Komanoya, T., Guha, S. K., Hara, K. & Fukuoka, A. 2011. Conversion of cellulose into renewable chemicals by supported metal catalysis. *Applied Catalysis A: General*, 409, 13-20.

[9] Moon, D. S. & Lee, J. K. 2012. Tunable synthesis of hierarchical mesoporous silica nanoparticles with radial wrinkle structure. *Langmuir*, 28(33), 12341-12347.

[10] Nakagawa, Y. & Tomishige, K. 2012. Production of 1, 5-pentanediol from biomass via furfural and tetrahydrofurfuryl alcohol. *Catalysis Today*, 195(1), 136-143.

[11] Parshetti, G. K., Quek, A., Betha, R. & Balasubramanian, R. 2014. TGA–FTIR investigation of co-combustion characteristics of blends of hydrothermally carbonized oil palm biomass (EFB) and coal. *Fuel Processing Technology*, 118, 228-234.